Sensors and Materials, Vol. 36, No. 5 (2024) 1805–1813
MYU Tokyo

S & M 3635

A Compact Tapered Antenna for Implanted Medical Biosensor Systems

Pei-Jung Tseng,[1] Ching-Fang Tseng,[2*] Pin-Yi Lee,[2] and Yu-Lin Cheng[2]

[1]Department of Pathology and Laboratory Medicine Taichung Veterans General Hospital, 1650 Taiwan Boulevard Sect. 4, Taichung, Taiwan
[2]Department of Electronic Engineering, National United University, No. 2 Lien-Da, Nan-Shih Li, Miao-Li 36003, Taiwan

(Received October 30, 2023; accepted March 12, 2024)

Keywords: tapered antenna, meandered strip line, implanted antenna

A compact tapered antenna with a meandered strip line for implanted biomedical applications is proposed. The proposed antenna can be operated at a medical device radio communication service (MedRadio) band, a long-term evolution (LTE) band 8, an LTE band 11, and an industrial, scientific, and medical (ISM) band. A linear tapered structure is introduced to improve antenna gain, and simultaneously, a meander line is adopted to lower the resonant frequency to the MedRadio band and reduce the size of the proposed antenna. The proposed compact tapered implanted antenna is fabricated and measured using a skin-mimicking gel. The measured results are in good agreement with the simulated ones. The proposed antenna has gain values of −15.55 and −8.37 dBi in MedRadio and ISM bands, respectively. Furthermore, the salient features of the proposed antenna make it a candidate for wireless biotelemetric applications.

1. Introduction

Recently, body area networks (BANs) have attracted widespread research interest because they can wirelessly and continuously monitor patients to improve the quality of medical services, thus making implantable devices popular. Implanted medical devices with integrated wireless sensors enable communication between internal and external devices through implanted antennas.

In today's patient care systems, implantable sensors are implanted into the human body to enable the continuous monitoring of body parameters, including blood pressure, blood glucose level, and intracranial pressure, and to communicate well with the external environment, allowing patients to be assured of a good quality of life.(1) To obtain the human body's critical physiological data, the implanted telemetry antenna plays an extremely important role. Implantable antennas with far-field RF telemetry communications offer the advantages of high data rate and long-distance communication. To maximize system performance at high data rates, the available bandwidth of an implantable antenna is an important parameter. For instance,

*Corresponding author: e-mail: cftseng@nuu.edu.tw
https://doi.org/10.18494/SAM4796

ISSN 0914-4935
https://myukk.org/

multichannel neural recording systems and visual prostheses require sufficient bandwidth to meet the high data rate requirement of 10 Mb/s. Implantable antennas operate at multiple frequency bands, but the medical device radio communication service (MedRadio; 401–406 MHz, 413–419 MHz, 426–432 MHz, and 438–444 MHz) and industrial, scientific, and medical (ISM; 433–438 MHz and 2.4–2.48 GHz) bands are the most common frequency bands.[2,3]

Developing implantable antennas inside the human body faces more challenges such as antenna miniaturization, impedance matching, biocompatibility with the surrounding tissue, and specific absorption rate (*SAR*). By considering human tissues with high permittivity (such as skin or brain) and applying antenna miniaturization methods (such as using pyramidal or meandering structures, employing multiple folded structures, introducing short circuits, and employing thick ceramic substrates with high permittivity), the implanted antenna size can be reduced.[4–6] However, the lossy and inhomogeneous human tissue causes most of the reported implantable antennas to have low gain. Recently, many antenna types with good gain have been manifested in applications. Among them, the tapered slot antenna is well known and can provide broadband impedance matching, planar configuration, good directivity, and reasonable gain owing to its gradual tapered structure.[7]

In this study, an implanted human skin antenna operating at MedRadio and ISM bands is proposed. To avoid signal attenuation by the human skin and body fluids, we adopt a linearly tapered structure to improve the implanted antenna gain. Moreover, a meander line structure is introduced to reduce the antenna size, which results from the MedRadio system operating at low frequencies. The design procedures, parametric analysis, and performance of the proposed antenna are investigated and presented below.

2. Antenna Design

An overview of the compact tapered implanted antenna is shown in Fig. 1. The radiating element of the proposed antenna consists of two linearly tapered monopole structures, a meander line, an I-shaped microstrip line, and a 50 Ω microstrip feedline, which are placed on one side of an FR4 substrate with a permittivity ε_r of 4.4, a thickness of 0.8 mm, and a loss tangent tanδ of 0.02 as shown in Fig. 1(a). The linearly tapered monopole structures are introduced to enhance the operating bandwidth and gain, the meandering element is used to reduce the size of the proposed implanted antenna, and the I-shaped microstrip is adopted to tune the resonant frequency. The rectangular ground plane [Fig. 1(b)] of 11 × *GL* mm^2 size is on the other side of the substrate, and its relative position is shown by the green dotted line in Fig. 1(a). The radiating element is covered with a 0.64-mm-thick Al_2O_3 layer with a dielectric constant ε_r of 9.8 and a loss tangent tanδ of 0.0087. Then, the proposed antenna is covered with biocompatible silicone to prevent direct contact between the human tissue and the antenna conductor layer. The overall volume of the proposed tapered implanted antenna is 25 × 25 × 1.44 mm^3. Figure 1(c) shows the one-layer skin simulation model of 100 × 100 × 24 mm^3 size, which is placed at the center of a radiation boundary box with dimensions of 300 × 300 × 300 mm^3. The proposed tapered implantable antenna is placed at a depth of 4 mm below the surface of the skin model. The electrical properties of the skin simulation model at 402 MHz and 2.4 GHz are a conductivity σ

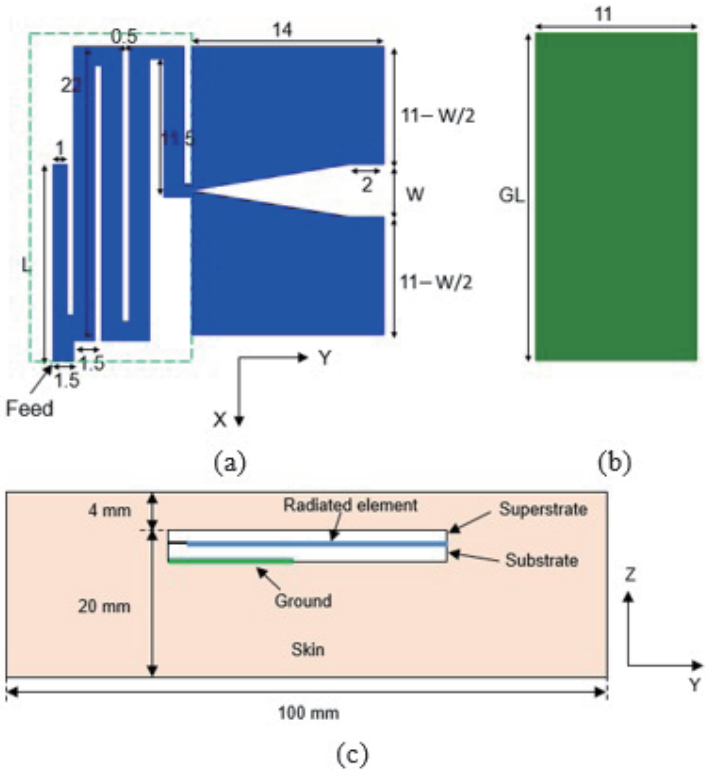

Fig. 1. (Color online) Proposed antenna geometry: (a) top view of the radiating element, (b) ground plane, and (c) side view of the antenna inside a homogeneous single-layer skin tissue structure.

of 0.689 S/m, and a dielectric constant ε_r of 46.7, and σ = 1.441 S/m, and ε_r = 38.1, respectively, as published in Ref. 8. Figure 1(a) shows the detailed geometric parameters of the proposed compact tapered implanted antenna.

3. Results and Discussion

The effects of the important design parameters, such as the slot opening width between two linearly tapered monopole structures (W), the length of the I-shaped microstrip line (L), and the length of the ground plane (GL), on the electric characteristics of the proposed antenna are described in this section. The length of the sum of the meander line and the tapered monopole structure is approximately a quarter wavelength at the lowest operating frequency, whereas the length of the I-shaped microstrip line corresponds to around a quarter wavelength at the highest operating frequency. Figure 2 shows the comparison of the return losses obtained with various slot opening width (W) values between two linearly tapered monopole structures. It can be clearly seen that the return loss of the 402 MHz band is mainly affected by W. By increasing W, the bandwidth of the 402 MHz band can be effectively improved. The largest bandwidth is obtained at W = 11 mm.

Figure 3 shows the simulated return losses of the proposed tapered implanted antenna obtained with different lengths of the I-shaped microstrip line. It can be seen that L mainly controls the high-frequency band. As L decreases, the resonant frequency increases, corresponding to a low-frequency resonant mode that remains almost constant.

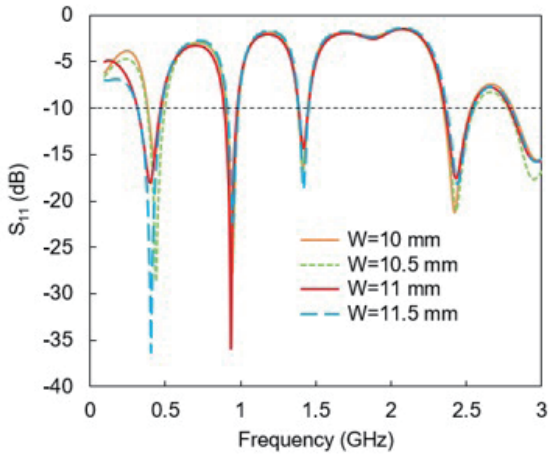

Fig. 2. (Color online) Simulated S_{11} of the proposed tapered implanted antenna for various slot opening width (W) values between two linearly tapered monopole structures.

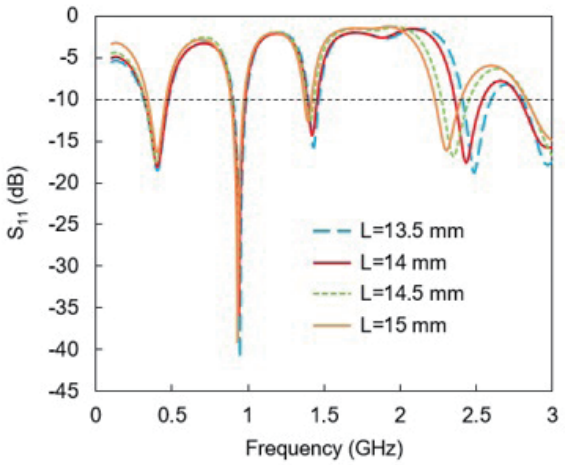

Fig. 3. (Color online) Simulated S_{11} of the proposed tapered implanted antenna for various length (L) values of the I-shaped microstrip line.

The effect of *GL* on the return loss curve of the proposed tapered implanted antenna is evaluated as shown in Fig. 4. *GL* increases from 21.5 to 25 mm. It can be found that *GL* contributes to improving the impedance matching and then enhancing the bandwidth characteristics of the ISM band for the proposed tapered implanted antenna. This result indicates that the bandwidth of the proposed antenna can be effectively improved by moderately adjusting the size of the ground plane, which is a phenomenon similar to the results described in Ref. 9.

The proposed antenna is fabricated and then fed by an SMA connector. To understand the *in vitro* testing performance of the proposed tapered implanted antenna, the recipes include 41.49% deionized water, 2.33% salt, and 56.11% sugar for the MedRadio band and 58.2% deionized water, 5.1% diethylene glycol monobutyl ether, and 36.7% Triton X-100 for the ISM band as mimicking gels provided by Refs. 10 and 11. In addition, the liquid mixtures of both mimicking gels are solidified using agarose. A comparison of the simulated and measured return losses is presented in Fig. 5, where W = 11 mm, L = 14.5, and GL = 22.5 mm. Overall good agreement can be observed between the measured and simulated return losses except for the higher frequency bands. This mismatch between the simulated and measured results could be due to imperfect surrogates for simulating the dielectric properties of the human skin over a wide frequency range resulting in differences in the dielectric constant and conductivity of the simulated materials and actual mimicking gels, as well as forming defects and solder roughness during fabrication. The −10 dB measured bandwidth is obtained at around 402 MHz, 900 MHz, 1.46 GHz, and 2.4 GHz with 274–448 MHz, 868.5–1013.5 MHz, 1.424–1.507 GHz, and 2.246–2.739 GHz, which simultaneously cover MedRadio, Long-Term Evolution (LTE) 8, LTE 11, and ISM systems, respectively.

The 3D radiation patterns of the proposed tapered implanted antenna at the operating frequencies of 402 MHz and 2.4 GHz are presented in Fig. 6. This figure shows that the proposed antenna has the main-direction radiation characteristic in the z-direction of the tapered structure,

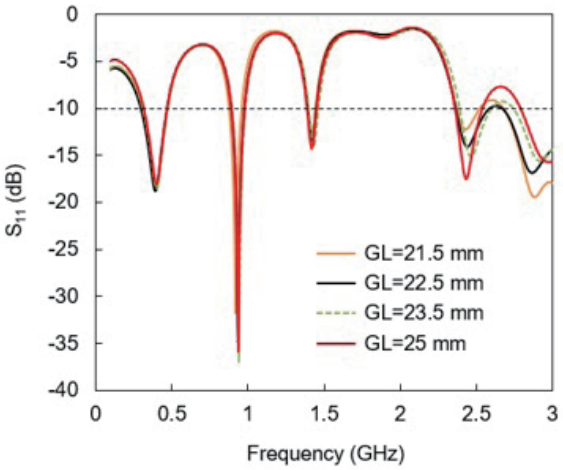

Fig. 4. (Color online) Simulated S_{11} of the proposed tapered implanted antenna for various GL values of the ground plane.

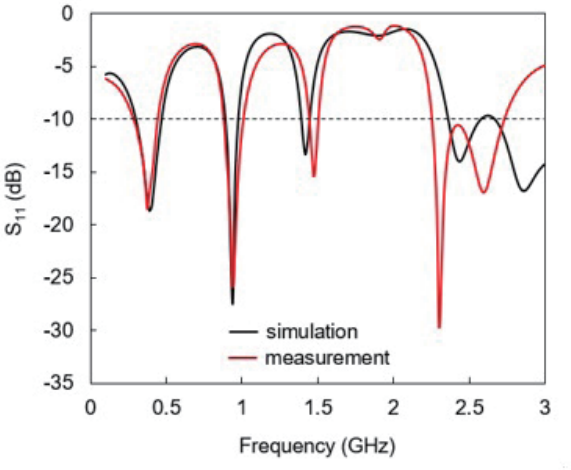

Fig. 5. (Color online) Simulated and measured S_{11} of the proposed tapered implanted antenna.

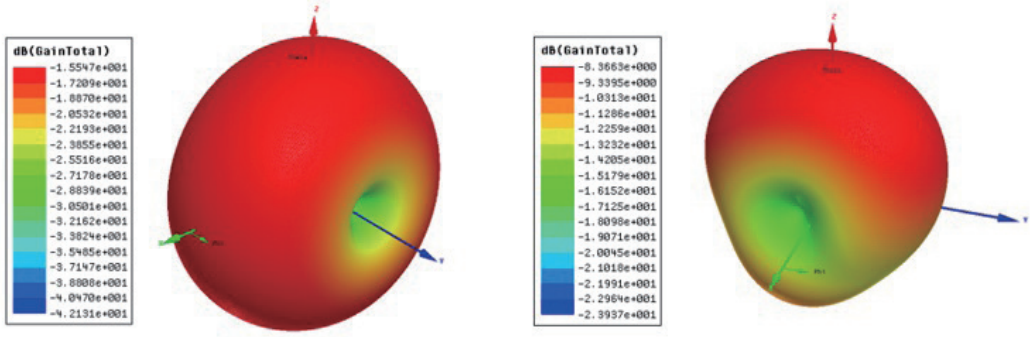

(a) (b)

Fig. 6. (Color online) 3D radiation patterns of the proposed implantable antenna at (a) 402 MHz and (b) 2.4. GHz.

especially at the higher frequency band. The measured far-field peak gains are −15.55 and −8.37 dBi for the MedRadio and ISM bands, respectively, whose small gain values are contributed by the lossy surrounding biological tissues. Then, further study is conducted on the effect of the slot opening width between two linearly tapered monopole structures (*W*) on the antenna gain. The comparison of gain values obtained with different *W* values in the design of the proposed tapered implanted antenna at 402 MHz (MedRadio), 900 MHz (LTE band 8), 1.46 GHz (LTE band 11), and 2.4 GHz (ISM) is shown in Table 1. Clearly, as W increases, the gain of the proposed antenna improves expected.

The specific absorption rate (*SAR*) is utilized to estimate the harmful effects of radiation from implanted medical devices, which restricts the maximum up to 1.6 W/kg over 1 g of tissue and 2 W/kg over 10 g of tissue according to IEEE C95.1-1999 and C95.1-2005 standards, respectively. The 1- and 10-g average *SAR* values on the radiating surface of the proposed tapered implanted antenna at 402 MHz and 2.4 GHz for 1 W input power are shown in Fig. 7.

Table 1
Antenna gains of the proposed implanted antenna obtained with different W values at 402, 900, 1460, and 2400 MHz.

Frequency (MHz)	Gain (dB)			
	$W = 10$	$W = 10.5$	$W = 11$	$W = 11.5$
402	−16.00	−15.91	−15.55	−15.07
900	−13.45	−12.11	−12.07	−11.89
1460	−11.86	−11.45	−11.04	−10.85
2400	−9.68	−8.45	−8.37	−7.47

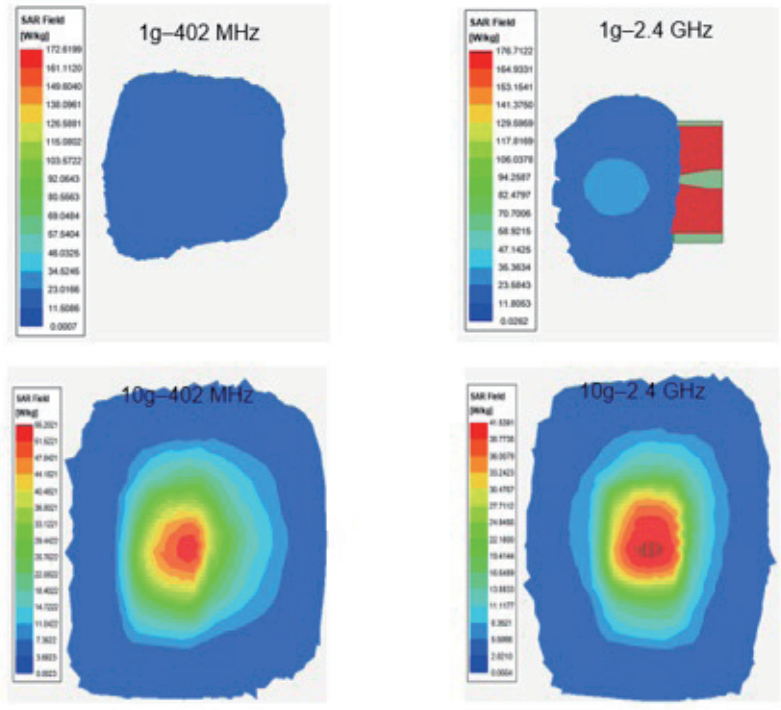

(a) (b)

Fig. 7. (Color online) 1- and 10-g average *SAR* distributions on the radiating surface of the proposed tapered implanted antenna at (a) 402 MHz and (b) 2.4 GHz for 1 W input power.

The highest *SAR* is found at the center of the radiating element, and the energy dissipated by thermal conversion gradually decreases away from the center of the antenna. For 1 W input power, the average *SAR* maximum values for 1- and 10-g standards are respectively 172.62 and 55.2 W/kg at 402 MHz. Moreover, the obtained *SAR* values are 176.71 W/kg for the 1-g standard and 41.54 W/kg for the 10-g standard at 2.4 GHz. After the input powers are limited to 9.2 mW for 1 g and 36.2 mW for 10 g at 402 MHz as well as 9 mW for 1 g and 48 mW for 10 g at 2.4 GHz, all the average *SAR* values can meet the IEEE standard.

Finally, the proposed antenna is compared with other implantable antennas designed in the recent year, for example, in terms of antenna size, operating frequency, gain, and *SAR*, as summarized in Table 2.[12–15] From Table 2, it is clearly confirmed that the use of the meander line and the tapered structure can realize a smaller size and a higher gain, respectively, although

Table 2
Performance comparison of implanted antennas in the MedRadio and ISM bands in recent studies.

Ref.	Substrate (ε_r/tanδ)	Volume (mm^3)	Frequency (MHz)	Bandwidth (MHz)	Gain (dBi)	*SAR* (W/kg)		Max. input power (mW)
						1-g	10-g	
12	Rogers 3010 (10.2/0.0023)	642.62	402	30	−36.7	832	—	3.8
			2400	170	−27.1	690	—	4.6
13	Rogers 3010 (10.2/0.0023)	797.96	402	150	−34.08	241.5	—	6.625
			2400	430	−15.2	149.7	—	
14	RT Duroid 5880 (2.2/0.0009)	3375	2400	900	−18.5	1101.7	—	1.45
			5800	1500	—	1135.8	—	1.41
15	FR4 (4.4/0.02)	6720	402	6	−31.7	—	—	5.186 (1-g); 30.17 (10-g)
			2400	45	—	—	—	—
This work	FR4 (4.4/0.02)	900	402	174	−15.55	172.62	55.20	9.2 (1-g); 36.2 (10-g)
			900	145	−12.07	—	—	—
			1460	83	−8.37	—	—	—
			2400	493	−8.37	176.71	41.54	9 (1-g); 48 (10-g)

the proposed antenna is fabricated on the FR4 substrate with low dielectric constant. Additionally, the *SAR* of the proposed implanted antenna can be effectively improved compared with those of other implantable designs because the antenna is encapsulated with a biocompatible ceramic aluminum oxide (Al_2O_3) material as the superstrate. The use of commercially available and biocompatible Al_2O_3 ceramics as the superstrate can separate the lossy high-dielectric-constant human tissue from the antenna conductor, limit the leakage current from the conductor directly entering the lossy material, and avoid the high-dielectric-constant human body from shorting out the antenna. In addition, the Al_2O_3 ceramic with a high dielectric constant of 9.8 and low loss characteristics meets the low-frequency operation of implantable antennas.[16,17] Therefore, the proposed tapered implanted antenna is a good candidate for biotelemetric applications owing to its features of simple fabrication, relatively small size, high gain, and low *SAR* values.

4. Conclusions

A compact tapered skin implanted antenna is presented in this paper. The tapered structure improves antenna performance and gain. The meander line is also utilized for antenna miniaturization. The return loss results indicate the measurement and simulation agreements. Moreover, the proposed antenna can generate 174, 145, 83, and 493 MHz impedance bandwidths covering the MedRadio band, LTE band 8, LTE band 11, and ISM band, respectively, as well as exhibit excellent gain, acceptable radiation characteristics, and improved *SAR* values to satisfy the IEEE standard safety guidelines.

Acknowledgments

This work was sponsored by the National Science Council of the Republic of China under grant no. MOST 110-2221-E-239-005.

References

1 X. Y. Liu, Z. T. Wu, Y. Fan, and E. M. Tentzeris: IEEE Antennas Wireless Propag. Lett. **16** (2017) 577. https://doi.org/10.1109/LAWP.2016.2590477
2 N. A. Malik, P. Sant, T. Ajmal, and M. Ur-Rehman: IEEE J. Electromagn. RF Microw. Med. Biol. **5** (2021) 84. https://doi.org/10.1109/JERM.2020.3026588
3 G. Kaur, A. Kaur, G. K. Toor, B. S. Dhaliwal, and S. S. Pattnaik: Biomed. Eng. Lett. **5** (2015) 203. https://doi.org/10.1007/s13534-015-0193-z
4 F. Merli, L. Bolomey, J. F. Zurcher, E. Meurville, and A. K. Skrivervik: Proc. 2011 5th European Conf. Antennas and Propagation (IEEE, 2011) 2487. https://ieeexplore.ieee.org/document/5782053
5 F. J. Huang, C. M. Lee, C. L. Chang, L. K. Chen, T. C. Yo, and C. H. Luo: IEEE Trans. Antennas Propag. **59** (2011) 2646. https://doi.org/10.1109/TAP.2011.2152317
6 T. F. Chien, C. M. Cheng, H. C. Yang, J. W. Jiang, and C. H. Luo: IEEE Antennas Wireless Propag. Lett. **9** (2010) 599. https://doi.org/10.1109/LAWP.2010.2053342
7 J. Eichenberger, E. Yetisir, and N. Ghalichechian: IEEE Trans. Antennas Propag. **67** (2019) 4357. https://doi.org/10.1109/TAP.2019.2906008
8 C. Gabriel, S. Gabriel, and E. Corthout: Phys. Med. Biol. **41** (1996) 2231. https://doi.org/10.1088/0031-9155/41/11/001
9 M. John, J. A. Evans, M. J. Ammann, J. C. Modro, and Z. N. Chen: IET Microw. Antennas Propag. **2** (2008) 42. https://doi.org/10.1049/iet-map:20070053
10 T. Karacolak, A. Z. Hood, and E. Topsakal: IEEE Trans. Microw. Theory Technol. **56** (2008) 1001. https://doi.org/10.1109/TMTT.2008.919373
11 T. Yilmaz, T. Karacolak, and E. Topsakal: IEEE Antennas Wireless Propag. Lett. **7** (2008) 418. https://doi.org/10.1109/LAWP.2008.2001736
12 Y. Liu, Y. Chen, H. Lin, and F. H. Juwono: IEEE Antennas Wireless Propag. Lett. **15** (2016) 1791. https://doi.org/10.1109/LAWP.2016.2536735
13 N. Ganeshwaran, J. K. Jeyaprakash, M. G. N. Alsath, and V. Sathyanarayanan: IEEE Antennas Wireless Propag. Lett. **19** (2020) 119. https://doi.org/10.1109/LAWP.2019.2955140
14 V. Kaim, B. K. Kanaujia, and K. Rambabu: IEEE Trans. Antennas Propag. **69** (2021) 1260. https://doi.org/10.1109/TAP.2020.3016483
15 A. Kiourti, J. R. Costa, C. A. Fernandes, and K. S. Nikita: IEEE Trans. Antennas Propag. **62** (2014) 2899. https://doi.org/10.1109/TAP.2014.2310749
16 P. Soontornpipit, C. M. Furse, and Y. C. Chung: IEEE Trans. Microwave Theory Technol. **52** (2004) 1944. http:// doi.org/10.1109/TMTT.2004.831976.
17 M. R. Robel, A. Ahmed, A. Alomainy, and W. S. T. Rowe: Electronics **9** (2020) 1099. http://doi.org/10.3390/electronics9071099

About the Authors

Pei-Jung Tseng received her B.S.M.T. degree from Fooyin University, Taiwan, in 2007 and her M.S. degree from the Graduate Institute of Biomedical Sciences, College of Medicine, Chang Gung University, Taiwan, in 2009. Since 2020, she has been a medical laboratory scientist of the Department of Pathology and Laboratory Medicine, Taichung Veterans General Hospital, Taiwan. Her research interest is in bioscience. (elenatseng0902@gmail.com)

Ching-Fang Tseng received her Ph.D. degree in electrical engineering from Cheng Kung University, Tainan, in 2007. Currently, she is a professor in the Electronic Engineering Department, National United University, Taiwan. She has been involved in the research and development of wearable and flexible antennas, implantable antennas, biomedical devices, microwave/mm-wave/sub-THz mobile antennas, wireless biosensors, glass-free ULTCC and LTCC microwave dielectric materials, biomedical signal analysis, nonintrusive biological signal measurement, and intelligent health monitoring systems. (cftseng@nuu.edu.tw)

Pin-Yi Lee received his B.E. and M.S. degrees from the Electronic Engineering Department, National United University (NUU), Miaoli, Taiwan, in 2021 and 2023, respectively. His main research interests are in bioengineering and the development of wireless communication antennas and sensors. (joe1000618@gmail.com)

Yu-Lin Cheng received his B.S. degree from the Electronic Engineering Department, National United University (NUU), Miaoli, Taiwan, in 2015 and his M.S. degree from National Taipei University of Technology, Taipei, Taiwan, in 2017. He is currently an engineer working for Phison Electronics Corporation. His research interests are in planar antenna design, high-frequency device design, bioengineering, and sensors. (U0022108@smail.nuu.edu.tw)